Applied Physics A (2025) 131:127
https://doi.org/10.1007/s00339-025-08253-z

High-temperature superconductor $YBa_2Cu_3O_y$: electrical properties and structural instability

A. E. Rabadanova[1] · S. Kh. Gadzhimagomedov[1] · D. K. Palchaev[1] · M. Kh. Rabadanov[1] · R. M. Emirov[1] · V. S. Efimchenko[2] · Zh. Kh. Murlieva[1] · Sh. P. Faradzhev[1] · N. M.-R. Alikhanov[1]

Received: 21 October 2024 / Accepted: 9 January 2025

Abstract
The temperature dependences of electrical resistance were measured four-probe method. The analysis of the continuous structural evolution of the $YBa_2Cu_3O_y$ superconductor using low-temperature X-ray diffraction have been performed. In the normal state, the dependences of the temperature coefficients of electrical resistance (α_ρ) on the volumetric thermal expansion (α_V) are close to linear with correlation coefficients (correspondence) $r \sim 0.98$. In the region of the transition to the superconducting state, the temperature dependences of αρ and α_V exhibit anomalies in the form of maxima and minima of the functions. For each phase, the onset of the superconducting transition is accompanied by lattice compression, after which the volume grows in the region of the T_c value of these phases on the $d\rho/dT$ dependence. In the region of transition to the superconducting state, significant changes in the degree of orthorhombicity are observed, in the form of its sharp increase to 0.01 and 0.009 at temperatures of 90 and 87 K, respectively. It is shown that the volume change ΔVs in the temperature region from ~92 to ~90.5 K is higher than for the interval from ~88 to ~87 K and amounts to 0.73% and 0.58%, respectively. An attempt has been made to consider the origin of superconductivity from a position that takes into account the peculiarities of lattice deformation formation, considering the $YBa_2Cu_3O_y$ lattice as a system of interacting polarized atoms, using Slater's ideas about the formation of elementary charge excitations in a condensed medium.

Keywords Superconductivity · HTSC · Low-temperature X-ray structural studies · Thermal expansion · Correlation

1 Introduction

High-temperature superconductors (HTSC), including compounds based on complex copper oxides doped by changing the oxygen content, have found wide practical application. They are promising for creating components for electric power and electronics [1], as systems based on Josephson contacts for quantum computers [2]. Interest in these materials is caused not only by practical applications, but also by fundamental research. Until now, establishing the nature of high-temperature superconductivity in them remains [3–5] one of the most important problems of condensed matter physics. Unlike metals, in these materials it makes sense to speak only of some charge excitations, with an insignificant degree of their generalization. To date, the issue of conductivity in the normal state, considered [3, 4] as the state of a "strange metal", has not been fully resolved.

The main difference between HTSC and low-temperature superconductors is the relatively high looseness of the packing, due to the significant contribution of the covalent bond. In this connection, it is obvious that it is important to consider the role of the crystal structure in the formation of conductivity and superconductivity, not only with a change in the degree of doping, but also the lattice parameters in the normal and superconducting states depending on the temperature.

A detailed study of the structure and properties of $YBa_2Cu_3O_y$ materials is devoted to the works [6–8]. With a decrease in temperature from room temperature to the transition temperature in $YBa_2Cu_3O_y$, anomalies of the crystal structure appear in the form of jumps in the lattice parameters and/or thermal expansion [9–16]. The anomaly near the temperature of ~ 140–180 K is usually associated [17] with the

✉ A. E. Rabadanova
rabadanova.aida@mail.ru

[1] Dagestan State University, Makhachkala 367008, Russia

[2] Institute of Solid State Physics of RAS, Chernogolovka 142432, Russia

Published online: 23 January 2025

presence of a pseudogap state. The anomalies are especially clearly recorded from the data of acoustic measurements [18, 19], showing the maxima of ultrasound absorption near ~ 140 − 180 and ~ 240–260 K. Clear changes in the lattice parameters and near T_c are observed for $YBa_2Cu_3O_y$ single crystals, where anomalies of the opposite sign, depending on the oxygen content, appear in the a and b directions [10]. The oxygen non-stoichiometry of $YBa_2Cu_3O_y$ is associated with mixed valences of copper in the basic plane, which determines the relationship between the oxygen content and the lattice parameters. The high conductivity observed in $YBa_2Cu_3O_y$ is indisputably linked to the increased population of labile oxygen atoms in the b direction and their ordered arrangement. This results in the deformation of lattice parameters and the phase transition from the tetragonal non-superconducting phase to the orthorhombic superconducting phase. It is clear that we must consider the role of thermal deformation of the lattice during the transition from the normal state to the superconducting state. The most effective method for identifying phase transitions that are temperature- and oxygen-dependent is to measure the coefficient of thermal expansion.

In particular, changes in lattice parameters with temperature changes (from room temperature to transition) have been studied with an ultrahigh resolution capacitive dilatometer [20] using relatively thick (typical thickness ~ 0.5 mm along the c-axis) twin crystals. The onset of superconductivity is accompanied by strongly anisotropic jumps in the expansion coefficients in the *a*-*b* plane, leading to changes in orthorhombicity. However, little effect is observed "along the *c*-axis direction" because the non-twinned crystals used (typical thickness of about 0.1 to 0.2 μm) were too thin to make reliable measurements.

Many works [21–23] have been devoted to studying structural parameters, such as lattice deformations, bond lengths and angles, displacements of individual ions within the unit cell in the YBCO system as a function of temperature. Studies of features in vibrational spectra during the transition to the superconducting state for superconductors are quite active [24–26].

Summarizing the conclusions of these studies it can be noted that the values of relative displacements of the nearest pairs of ions inside the unit cell in superconductors are anomally changed. In particular, we can note the increase of disorder in the Cu-O bond length with decreasing temperature [23]. In this regard, it is particularly important to determine the positions of oxygen atoms responsible for charge transfer from the reserve layer to the conducting layer. However, the exact determination of bond lengths and angles in the unit cell is a rather difficult task. At the same time, the accuracy of determining the coordinates of oxygen atoms is low because of the weak ability of oxygen atoms to scatter X-rays, compared to other cations in the system [22].

Summarizing the conclusions of these works, we can establish that the cause of the high transition temperature is the instability of the crystal lattice and/or abnormal behavior of the phonon spectrum. In this case, for the explicit detection of characteristic anomalies, particularly thermal expansion, it is necessary to produce high-quality samples based on YBCO with a given structure and properties. Therefore, the novelty of this work consists in the fabrication and study of optimally oxygenated samples based on YBCO with phases close in oxygen content that show signs of preferential crystallite orientation along the *c*-axis. This allows us to carry out precision X-ray diffraction studies of the thermal lattice deformation for the YBCO sample in the superconducting state and to detect lattice anomalies for each of the phases based on oxygen content. The temperature dependence of electrical resistivity is a sensitive parameter to the thermal deformation of the lattice. What is new in this work is an attempt to consider the emergence of superconductivity from a perspective that takes into account the peculiarities of lattice deformation, considering the $YBa_2Cu_3O_y$ lattice as a system of interacting polarized atoms. This approach uses Slater's ideas about elementary charge excitations in a condensed medium. The effects of excitation and relaxation of elementary charge excitations in the system of interacting polarized atoms are accompanied by the work to move the system away from equilibrium and back to a new equilibrium state after thermal action. Consequently, studying volume changes resulting from phase transformations in high-temperature superconducting materials is important. It is quite a difficult task to accurately determine bond lengths and angles in the unit cell for each of the phases close in oxygen content.

The studies performed in this work aim to consider various changes in crystal structure and set the functional properties of the materials, demanded in practice. The research provides a new impetus for establishing the nature of HTSC superconductivity and their conductivity in the normal state, as well as developing technologies for producing HTSCs with specific characteristics.

The issues of predicting new superconducting materials with given characteristics and high values, remain one of the key issues in condensed state physics. In particular, the superconducting transition temperature significantly depends mainly on the oxygen content and alloying additives in the materials, which is manifested through changes in their lattice parameters. The authors of the present work previously [27] made an attempt to predict the superconducting transition temperature from the temperature coefficient of resistance before the transition for YBCO samples in nanostructured form. In [28, 29], superconducting

transition temperature prediction models have been developed for YBCO and MgB_2 systems based on lattice parameters. Although these prediction approac In this regard, the goal of this work was to conduct X-ray diffraction studies of the thermal transformation of the lattice for the $YBa_2Cu_3O_y$ sample, within only a few close oxygen phases, in normal and superconducting states.hes lead to efficient and inexpensive estimates of the superconducting transition temperature using empirical dependence [27] and based on lattice parameters [28, 29], but it is not clear why exactly at a certain temperature the transition occurs. Therefore, an attempt to estimate the electrical properties, including the temperature of the superconducting transition according to the thermal deformation data and, vice versa, to judge the changes in interatomic distances by changes in electrical properties. Since the temperature dependence of electrical resistivity is a sensitive parameter to the thermal deformation of the lattice, so the emergence of superconductivity should be considered from a position that takes into account the peculiarities of the formation of lattice deformation. These results can be used to predict new superconducting materials with specific characteristics and high values of T_c, higher than currently achieved.

Consequently, the objective of this study was to perform X-ray diffraction analysis on the thermal lattice deformation of the $YBa_2Cu_3O_y$ sample, which contains multiple close oxygen phases, in both the normal and superconducting states.

2 Methods and materials

The $YBa_2Cu_3O_y$ -based samples were prepared using the solid-state reaction method. Despite the simplicity and efficiency of traditional ceramic technology involving solid-phase synthesis and many years of experience in producing YBCO in different laboratories around the world, there are still no universal methods. The production of quality samples based on YBCO with a specific structure and properties significantly depends on the technological methods of synthesis, sintering and processing.

In the present work, dense (~6.1 g/cm^3), optimally oxygenated samples based on YBCO with phases close in oxygen content, showing signs of preferential orientation of crystallites along the c-axis, were fabricated. After prolonged stirring in agate mortar for 10 h of initial powders of Y_2O_3 (~99.9%, Sigma-Aldrich), $BaCO_3$ (~99.9%, Sigma-Aldrich) and CuO (~99.9%, Sigma-Aldrich) compositions, weighed in stoichiometric ratio, with addition of alcohol, provided homogeneous distribution of initial components during synthesis, at the first stage (the content of the main phase according to XRD data after synthesis was not less than 90%). This mixing resulted in the ultra-dispersity of the initial reagents, increasing the number of nuclei due to geometric factors (homogenous distribution of particles and a larger number and area of contact between particles). Subsequently, thorough grinding of the ceramics, mixing with alcohol after the first and second stages, and sintering provided homogeneity and recrystallization of the grains, resulting in an increase in density. During pressing, the directional deformation provides a marked direction of grain packing and during sintering there is an oriented growth of grains, i.e. a texture is formed (preferential orientation is confirmed by structure studies). Sintering was carried out in three stages at 870 (stage 1, synthesis), 900 (stage 2) and 910 ºC (stage 3) for 10 h in a Nabertherm muffle furnace, providing homogeneous heating of ceramics in six planes, oxygen saturation at each stage was carried out in air at 450 ºC for 5 h. This technology provided a reduction in the synthesis temperature, sintering temperature and the number of steps.

Rectangular samples measuring approximately $5 \times 2 \times 2$ mm were cut out for the study from 20 mm diameter and 3 mm thick tablets.

The temperature dependences of electrical resistance were measured using a standard four-probe method with an automated stand based on a Keithley 2002 digital multimeter. Current and potential contacts were created by applying silver paste to the sample surface. Contact treatment at 200 °C allowed us to obtain a contact resistance of less than 1 Ω. To eliminate the influence of parasitic signals, measurements were performed in the temperature drift mode when switching the directions of the transport current.

X-ray structural analysis for the powder obtained by grinding the ceramics after the third stage was performed in a wide temperature range (from room temperature to superconducting temperatures) on a SIEMENS D-500 powder diffractometer with a cryostat down to 82 K. The samples were loaded at room temperature with subsequent cooling to the desired temperature. The imaging was performed on a single-crystal silicon substrate with a sample well size of 15×20 mm. Scanning was performed using $CuK\alpha_{1,2}$ X-ray radiation, without a secondary monochromator, in the 2θ angle range from 5 to 90° with a step of 0.02 and a time exposure of 12 s at each point. For thermal equilibrium, each temperature was maintained for about 5 min before the measurement. The crystal structure analysis was performed using the High Score plus software package. The accuracy of determining the lattice parameters was ~10^{-3} nm.

3 Results and discussion

3.1 Structure and electrical properties

Figure 1a shows the diffraction pattern of the sample taken at room temperature, as well as the results of the structural analysis using the crystal structure model from the ICSD database (PDF-2) No. 98-003-9359: space group Pmmm, Y (½½½), Ba (½½ 0.1851), Cu1 (0 0 0.3557), Cu2 (0 0 0), O1 (0 ½ 0), O2 (0 ½ 0.3778), O3 (½ 0 0.3776), O4 (0 0 0.1600) [30]. The following discrepancy coefficients were achieved: weighted profile ωRp = 5.07%, profile Rp = 3.7433%, "goodness of the fit" $\chi^2 = 1.39$, Bragg coefficient $R_B = 3.64\%$. Based on the refinement results, the following crystal cell parameters were obtained: $a = 3.8236$ Å; $b = 3.8862$ Å; $c = 11.6854$ Å; $V = 173.6397$ Å^3. The diffraction pattern contains minor peaks corresponding to the Y_2BaCuO_5 (Y-211) and $BaCuO_2$ phases, the content of which is ~3%. For $YBa_2Cu_3O_y$, the oxygen index calculated using the empirical relationship: $y = 7 - \delta = 75.25 - 5.856 \times \boldsymbol{c}$, where "***c***" is the lattice parameter along the c axis [31], was ~6.9. This y value is consistent with the oxygen content determined from the superconducting transition temperature (T_c). The T_c parameter was determined using the results of measurements of the temperature dependence of electrical resistance.

Figure 1b shows the temperature dependence of the electrical resistance of the YBCO sample. The value of y, estimated from the T_c(y) dependence [8], is ~6.87– ~ 6.82. Such a high value of y is an indicator of the optimal oxygen content in the YBCO structure with almost completely occupied O(1) positions in the CuO chains along the *b*-axis. The observed metallic behavior of the $\rho(T)$ dependence from 300 to 100 K is typical of an optimally saturated YBCO sample; the electrical resistance value at 300 K is $\sim 5 \cdot 10^{-3}$ Ohm·cm. The temperature of the pseudogap state T^* is about ~160 K. In this case, the onset of the transition ($T_{c,\,on}$) is ~ 92.8 K, which corresponds to the optimal value of T_c, and the width of the transition is approximately 7 K (Fig. 1c). This indicates the heterogeneity of the distribution of superconducting phases with different y values over the volume of the original sample.

The transport properties of YBCO ceramics are sensitive to the fraction of the superconducting phase, the content and ordering in the oxygen phase, and the properties are also significantly affected by violations of the packing density, defects, boundaries between grains and their purity [32–34]. The YBCO ceramics obtained in the work in several stages (see above) is presented as a system including a large number of pseudo-single-crystal domains with sizes greater than 40 μm, providing a certain degree of grain texturing [35].

For YBCO superconductors, the dependences of T_c on the oxygen content and the doping level *p* are well known, but the relationship of the critical current j_c on these parameters is ambiguous [36]. This is due to the fact that the complex microstructure determines the magnitude and nature of the current j_c from the temperature and field. The doping level *p* and j_c change from the oxygen content in the Cu-O direction, determining, in turn, the packing defects, i.e. are determined by the distortions of the structure by oxygen. Based on the empirical dependence of j_c on defects given in [36], the fraction of stacking faults f_{124}, in the form of additional Cu-O layers in YBCO, is estimated and is $f_{124} \sim 0.82$ at $p \sim 0.132$ for ceramics with a high degree of texturing. The doping level p was estimated based on the $T_{c,\,off}$ value, using the $T_c(p)$ expression from [8]. Figure 2 shows the I-V characteristics at different temperatures, the dependences of the current density j_c and the activation energy on the temperature in the region of the transition to the superconducting state for ceramics YBCO. The magnitude of the electric current at 82 K (for which the voltage is 0.01 mV) is 0.033 mA. With a decrease in temperature from 88 K to 82 K, the current j_c increases by ~11 times, but the increase in the value of j_c in the region of 88÷85 K is insignificant (no more than ~2 times). The maximum value of j_c at 82 K is ~421 A cm^2. The value of j_c estimated from electrical properties is usually an order of magnitude lower than the value measured from magnetic properties [37].

The activation energy *E*(T) in the region of the transition to the superconducting state was estimated using the expression:

$$\rho\,(T) = \rho_0 \exp(-E(T)/k_B T)$$

As can be seen, the results of the study of the E(T) dependence confirm the 3D behavior of ceramics, i.e. it is described by a quadratic dependence in the transition region. In a zero magnetic field, an increase in the defectiveness of the sample structure leads to a decrease in the absolute values of the activation energy [27, 38].

The diffraction patterns at low temperatures (from 300 to 82 K) for the obtained YBCO sample are shown in Fig. 3. With a change in temperature, only peaks corresponding to the rhombic structure (Pmmm) from the planes 002, 003, 102, 013, 110, 113, 200, 123, 220, 033, 226 are observed. Based on the data on the broadening of the diffraction peaks, the size of the coherent scattering region (crystallite size) and the values of microstrains were estimated using the method from [39], using the High Score Plus program. The crystallite size and the value of microstrains for all temperatures do not change significantly. In particular, at temperatures of 300 K, 90.5 K and 84 K the crystallite size (in nm) and the value of microstrains (in %) are ~80 nm (~0.15%), ~ 131.8 nm (~0.22%) and ~95.6 nm (~0.11%). For clarity of the study of the effect of temperature on the

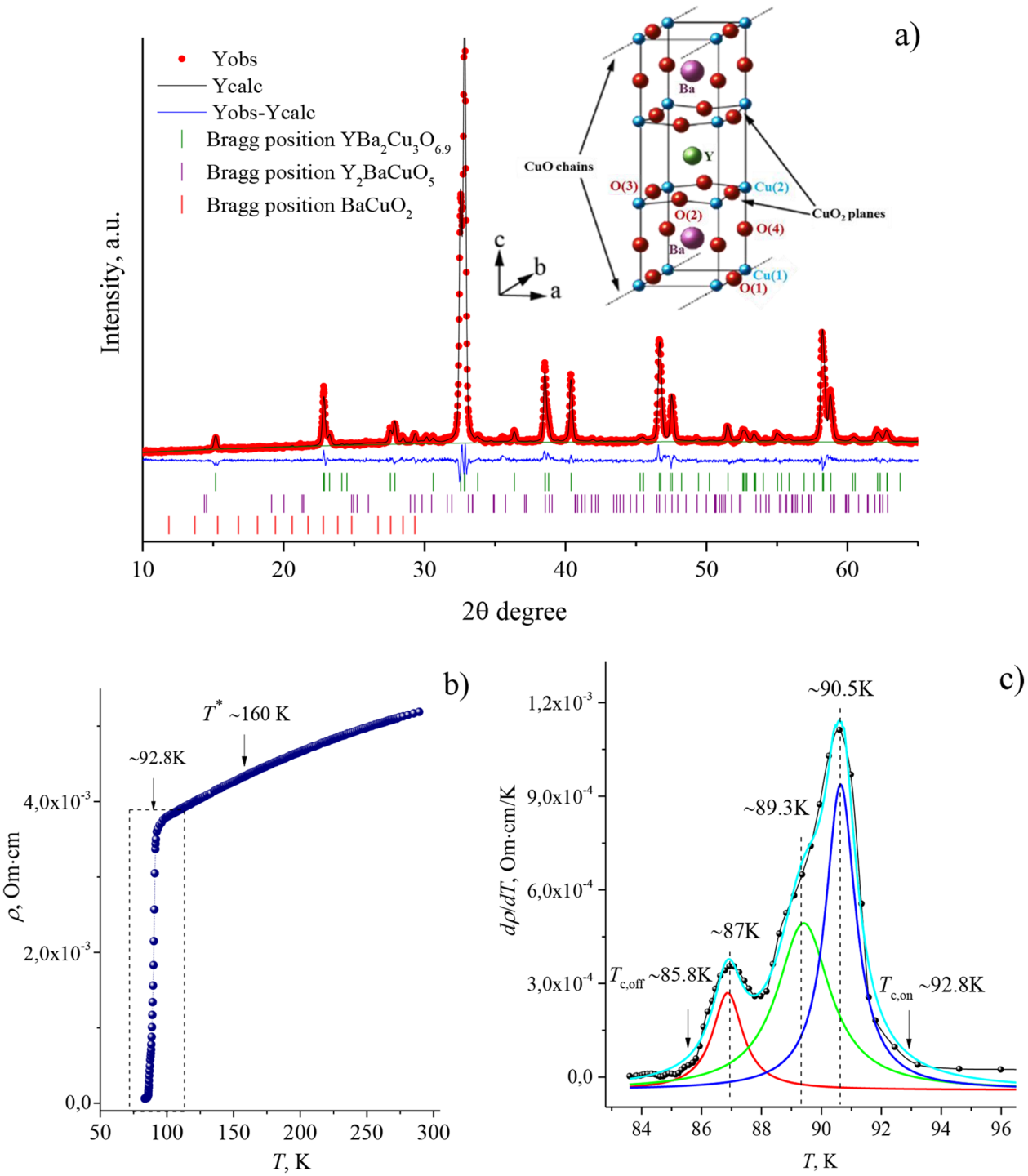

Fig. 1 Experimental (red), calculated (black) and differential (blue) diffraction patterns at room temperature – **a)**; temperature dependence of electrical resistance for the YBCO sample – **b)** and dρ/dT on T in the region of the transition to the superconducting state – **c)**

lattice parameters, Fig. 3 on the right shows an enlargement of some peaks and planes: 32.7° (013), 32.9° (110) and 46.8° (006+020). The intensity of the peaks (006), (020) and (200), containing mainly oxygen, is maximum, which is probably due to the ordering of oxygen in these planes. The peaks had a complex shape, indicating the existence of several phases with different oxygen contents in the sample. As can be seen, with a decrease in temperature to 93 K, a shift of the peaks towards larger angles is observed, i.e. lattice compression (Fig. 3 on the right). The shift in the opposite direction occurs when the temperature reaches 90.5 K, which indicates the expected increase in volume during the

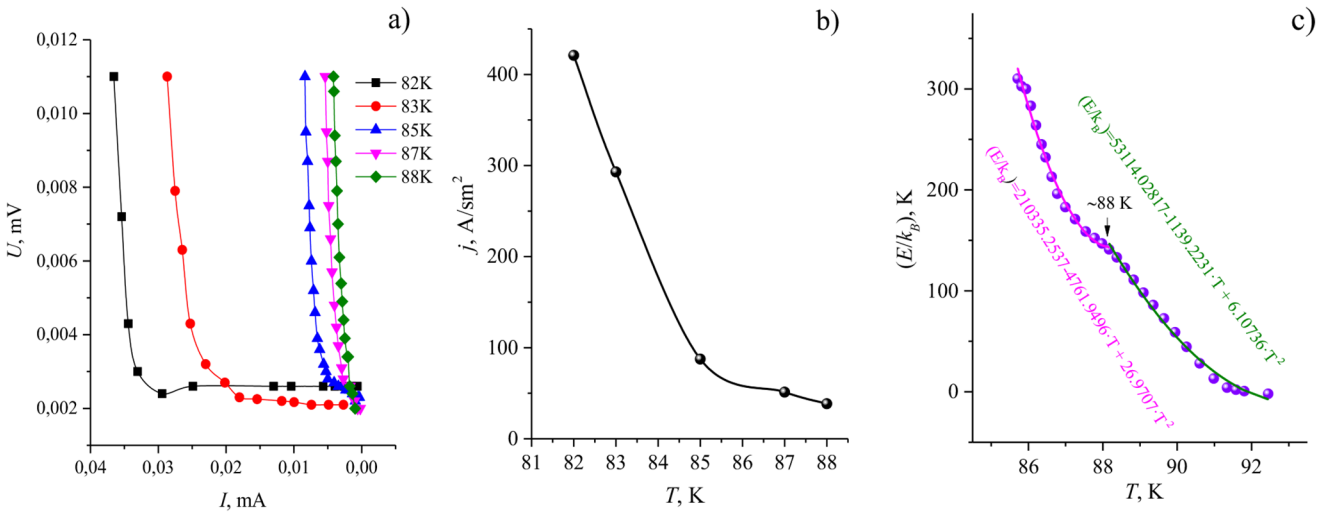

Fig. 2 Volt-ampere dependence – **a)**, current density – **b)** and activation energy – **c)** of a YBCO sample in the superconducting state

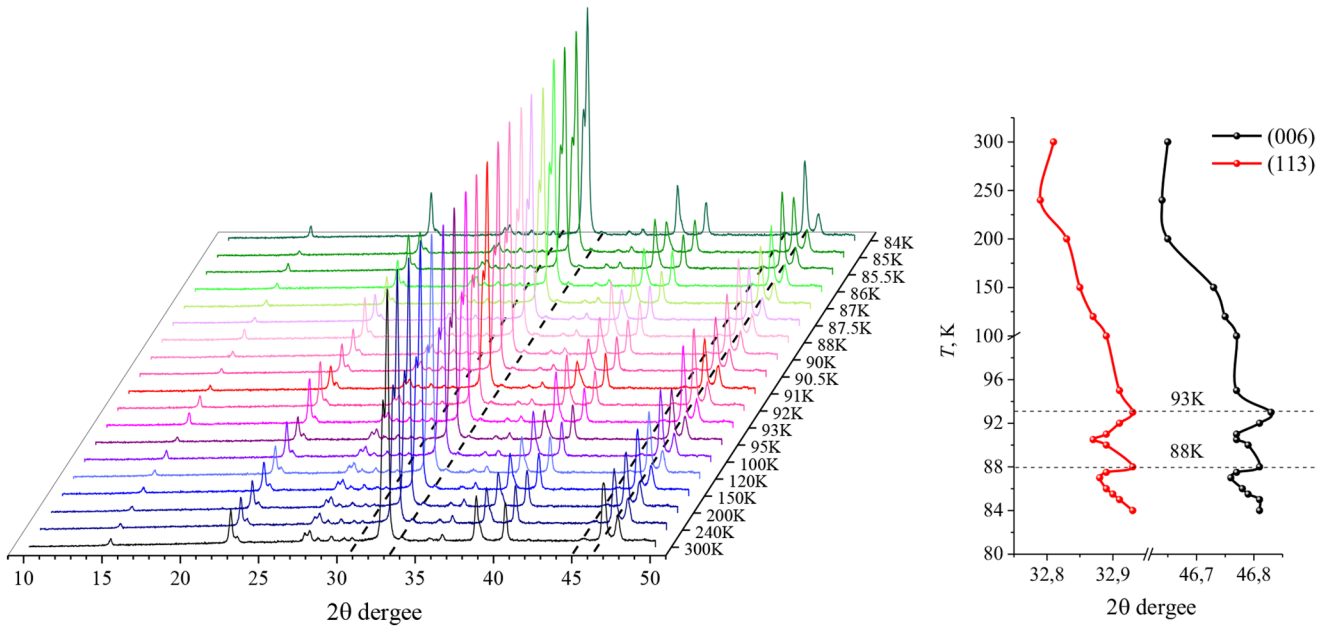

Fig. 3 X-ray diffraction patterns of a YBCO sample studied from room temperature to 82 K

transition to the superconducting state. A similar shift is observed when the temperature decreases to 87 K, which corresponds to the presence of several superconducting phases in the sample. It is known [40] that the asymmetry of the diffraction peak profile is associated with the peculiarities of the crystallite size distribution for polycrystalline materials. In this connection, it is necessary to perform a correct analysis of the results.

To isolate the exact position of the overlapping peaks (006) and (020), the integral intensities were refined by the separation method using the Lorentz function. The observed redistribution of intensities is due to the fact that the peak intensities are affected not only by the dynamic displacement of atoms (phonon spectrum), but also by changes in the static positions of atoms within the complexes [41].

Figure 4 shows X-ray reflections in the 2θ region from 46.6 to 47.6 from the (006), (020) and (200) planes, for which CuKα_2 was removed, leaving the diffraction from the 1.5406-A Kα_1 line, and the angle of their displacement at temperatures of 300, 92, 90.5 and 84 K. As can be seen, for all peaks not only changes in intensity are observed, but also shifts depending on temperature. The dependence of the shift angle on temperature has a characteristic maximum in the region of ~ 92 K for all peaks (006), (020) and (200). That is, the greatest shift of the peaks depending on temperature occurs at a value corresponding to $T_{c,\,on}$.

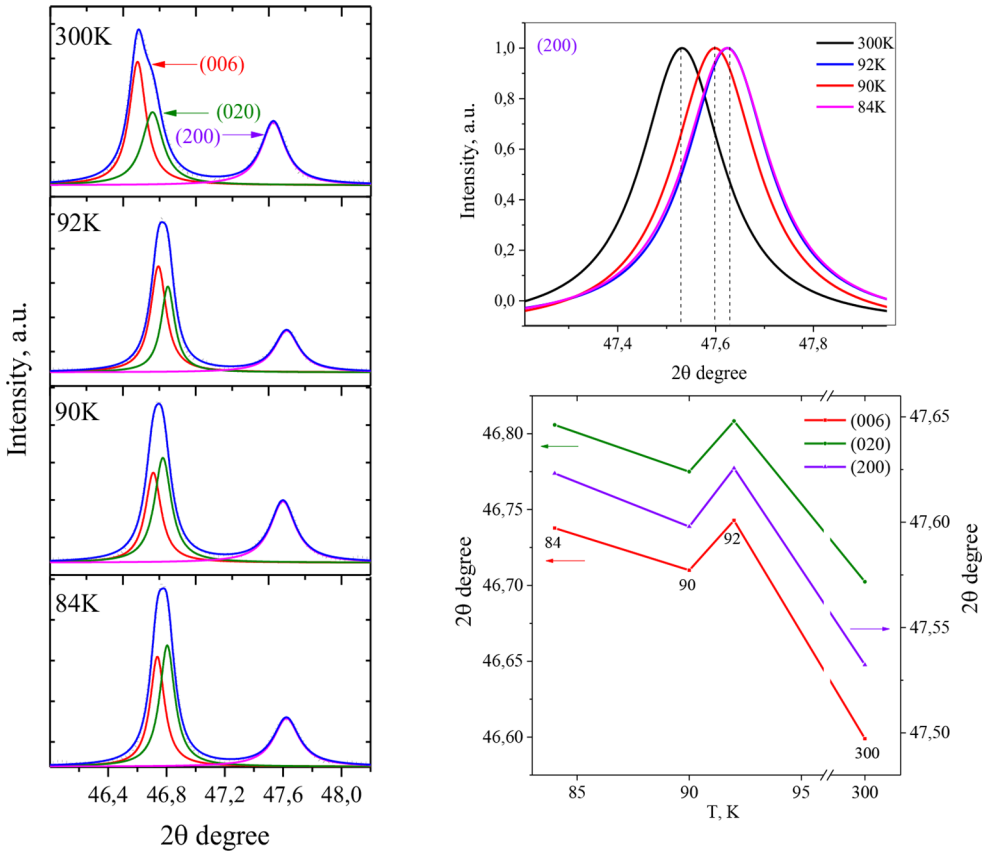

Fig. 4 Radiographs of a selected region of 2θ angles for different temperatures and the dependence of the displacement angle on temperature

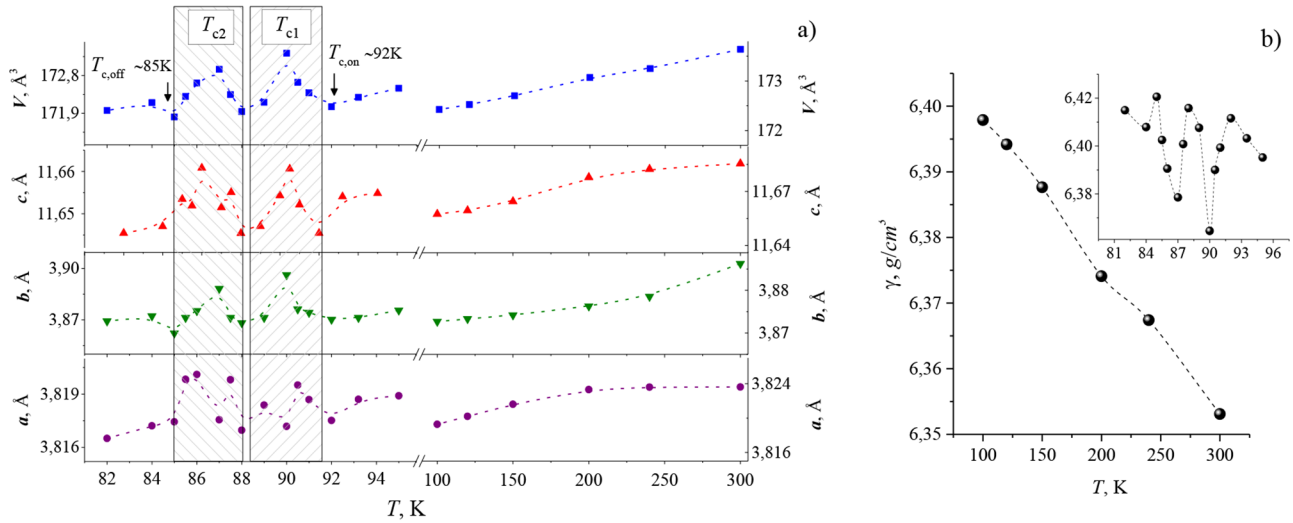

Fig. 5 Changes in lattice parameters and volume – **a**) and density – **b**) of the YBCO unit cell depending on temperature

Anisotropic change in peak intensities depending on crystallographic directions suggests that the relationship between the phonon and electron spectra in different directions can also be anisotropic [41]. With further decrease in temperature from ~92 K, coinciding with the value of $T_{c,\,on}$, an anomalous change in the density γ begins (Fig. 5). The maxima of the γ(T) dependence fall on the extreme points at 92 K, 88 K and 85 K. In this case, the lowest density (~6.36 g/cm^3) falls on the value of 90 K, which is practically comparable with the value at 300 K. This abrupt decrease in the value of γ to 90 K is associated with a sharp increase in volume (up to ~173.3 Å^3) at this temperature, coinciding with the first maximum on the derivative with respect to electrical resistance dρ/dT.

The region from ~92 to ~82 K, where anomalies appear in the $V(T)$ dependence, coincides with the width of ΔT_c on $d\rho/dT - T$. The values of the abrupt increase in V at ~90 K and ~87 K are consistent with the T_c values for different phases by oxygen content (~90.5 K and ~87 K, according to the $d\rho/dT$ dependence on temperature). In this case, the maximum change in volume occurs at ~90 K. The nature of the change in the lattice parameters (a, b, c) for perovskite structures is mainly determined by the deformations of the corrugated bonds (compressibility in directions).

Figure 6a shows the results of the change (in %) of the lattice parameters and volume with temperature. The values (Δa, Δb, Δc and ΔV) were estimated using the expression $((x_i\text{-}x_0)/x_0)$ 100%, where xi is the value of the quantity at a given temperature, x_0 is the value of the quantity at a temperature of 100 K. As can be seen, with a decrease in T from ~300 K to ~100 K, the parameters Δb and Δc change by ~0.35 and 0.25%, respectively, and the value of ΔV changes by approximately 0.7%. In this case, the change in the value of Δa, in contrast to the parameters Δb and Δc, is almost two times smaller and amounts to ~0.12%, which is characterized as anisotropic expansion. The data presented in this work (Fig. 6b) are in good agreement with the literature [14, 42, 43, 44] values (changes of the order of ~0.6%). All the curves of ΔV versus T are close to linear dependencies. However, an exception is the $\Delta V - T$ dependence of the authors [35], which is close to parabolic, coming through the minimum of the function at a temperature of ~150 K, corresponding to the pseudogap state.

3.2 Correlation analysis

Figure 7a shows the results of the correlation analysis of the temperature coefficients of resistance and volume expansion (α_ρ and α_V) for two intervals from ~290 K to ~140 K (in the normal state) and from ~120 K to ~95 K (in the pseudogap state). The values of α_ρ and α_VVare determined using the expressions $\alpha_\rho = d\rho/\rho dT$ and $\alpha_V = dV/VdT$. The inset shows the dependence of $1/\rho$ on T for the selected temperature interval. The temperature regions were determined by the deviation of this function from linear. The dependences of $\alpha_\rho(T)$ on $\alpha_V(T)$ for two intervals are close to linear with the correlation coefficients r up to the pseudogap state of ~0.992 and in the pseudogap state of ~0.977.

Figure 7b shows the temperature dependences of α_ρ and α_V in the region of the transition to the superconducting state. As can be seen, the curves contain irregularities in the form of maxima and minima of the functions, the number of which is consistent with the changes (with extremum points) in the dependence of $d\rho/dT$ on T. The samples produced in this work are quite dense and showed signs of preferential orientation of crystallites along the c-axis, but there is still a high defectivity of the structure, since the samples were obtained by prolonged mixing of powders in an agate mortar for 10 h at each stage (total duration of 30 h). For such defective samples, the number of nano-crystallites increases significantly and, consequently, the probability of existence of oxygen superconducting phases increases. This leads to an increase in the character of 3D behavior of conductivity and a decrease in the effect of transition to the pseudo-slit state. I.e. there is a violation of the transition from the state of "strange metal" to the pseudo-slot state. This effect is explained by the distortion of the nanoparticle structure, which leads to a change in the architecture of electrostatic fields created by the dipole moments of ions.

Control of the ordering of cations in the crystal lattice mainly ensures the production of materials with specified properties. The fundamental properties of superconductors

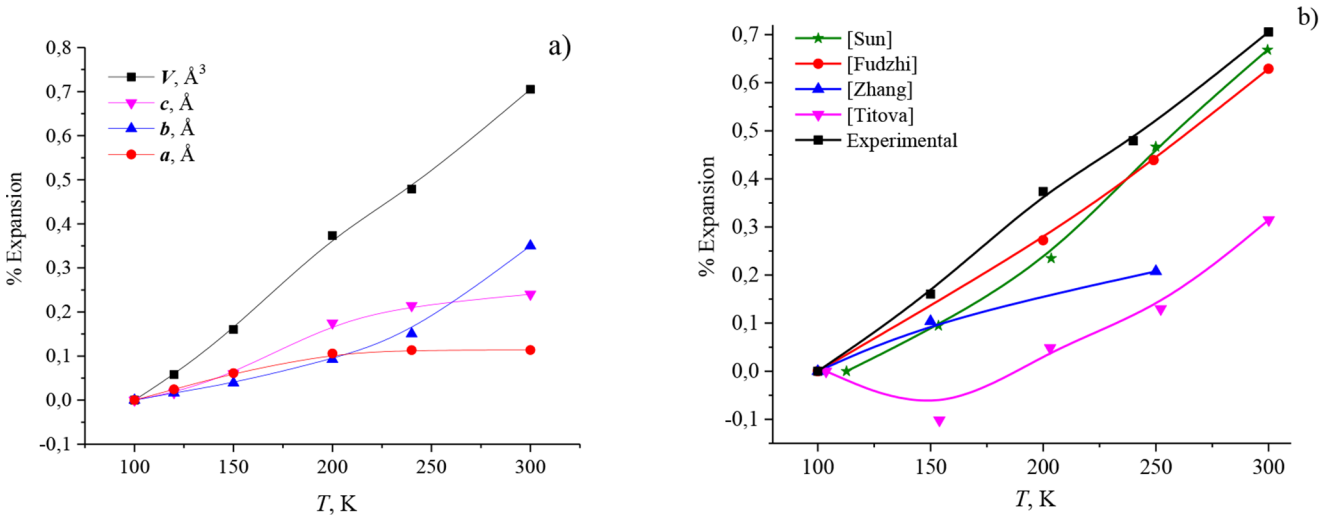

Fig. 6 Changes in the lattice parameters and volume of the YBCO unit cell depending on temperature – **a)** and comparison of the volume change for YBCO from different authors [14, 33, 34, 35] – **b)**

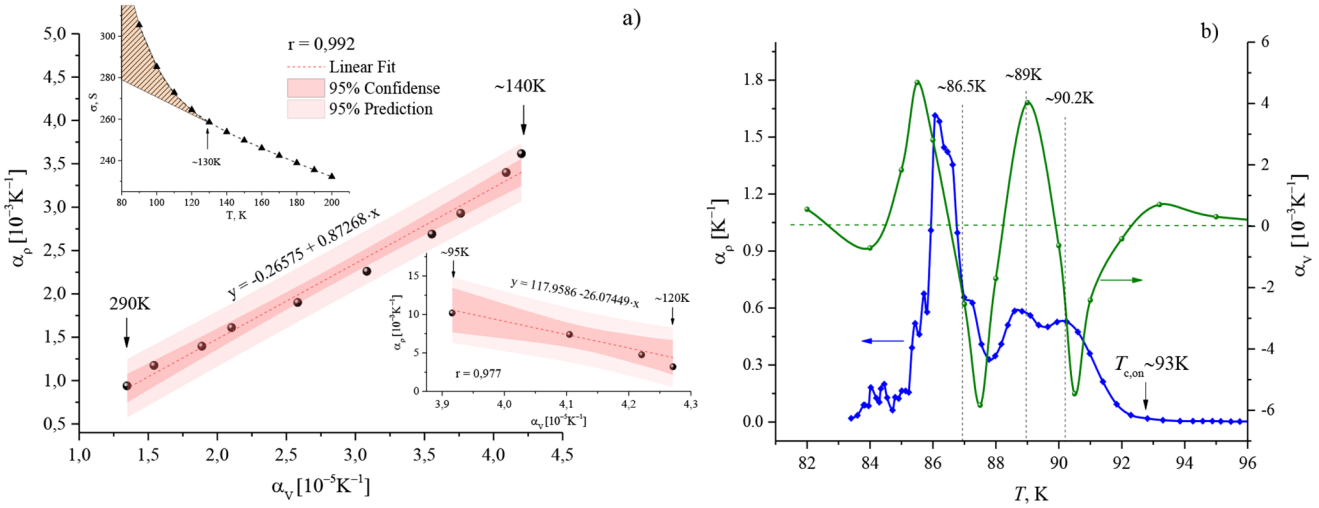

Fig. 7 Dependences of α_ρ on α_V in the normal state – **a)** and temperature dependences of the thermal expansion coefficient and temperature coefficient of resistance in the region of the superconducting transition – **b)**

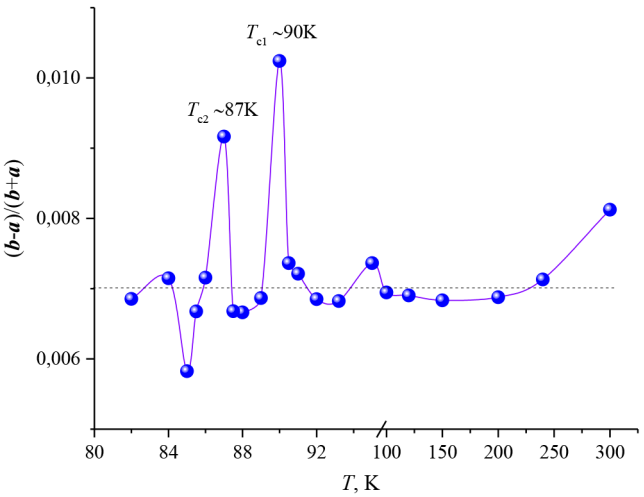

Fig. 8 Orthorhombicity parameter depending on temperature

are determined: at the microscopic level - by the degree of organization of local environments (distortions), the size of crystallites and their defects; at the macroscopic level - by crystallite ensembles, porosity and the proportion of cracks. Changes in the crystal lattice upon cooling, in the form of compression and stretching, ensure the nature of the localization of charge carriers, thereby, in general, setting (changing) the electronic structure of the sample (the density of electron states) [44, 45]. Figure 8 shows the temperature dependence of the parameter that determines the degree of lattice orthorhombicity $(\boldsymbol{b}\text{-}\boldsymbol{a})/(\boldsymbol{b}+\boldsymbol{a})$, which is a function of the charge carrier concentration.

At room temperature, the degree of orthorhombicity is ~ 0.008, which is close in value to the parameters known in the literature. With a decrease in temperature to 250 K, an insignificant decrease in the degree of orthorhombicity to a value of ~ 0.007 is observed, the value of which is maintained up to the superconducting transition temperature. At the same time, significant changes in the degree of orthorhombicity are observed in the region of the transition to the superconducting state - at temperatures of 90 and 87 K, a sharp increase in the parameter to 0.01 for T_{c1} and 0.009 for T_{c2}, respectively, occurs. It is evident that an anomalous change in the degree of orthorhombicity is observed in the region above and below the average values of ~ 0.007 during the transition to the superconducting state (dotted line, see Fig. 8), thereby indicating a significant change in the degree of localization of charge carriers with a decrease in temperature and setting T_c, which, in general, is reflected in the properties. Changes in the cation composition and oxygen index lead to orthorhombic lattice deformations in YBCO [46]. The authors in [47] suggest that orthorhombic deformations are determined by an "independent stability loss mechanism". If the change in the degree of orthorhombicity is related to the number of oxygen atoms in the unit cell of YBCO, located in the positions O(1a) (1/2,0,0) and O(1b) (0,1/2,0) [48]. However, in the samples the oxygen content in positions O(1a) and O(1b) remains unchanged, then we can assume that the change in this parameter temperature dependence occurs mainly as a result of lattice distortion, for example, octahedrons CuO_6 in the unit cell [22] Therefore, it is unambiguous to note that these anomalies of the parameter are entirely due to superconductivity, and not any additional structural effects. This is confirmed by the fulfillment of the thermodynamic Ehrenfest relation linking the expansion anomalies to the anomaly in specific heat capacity and the pressure (stress) dependence on temperature T_c.

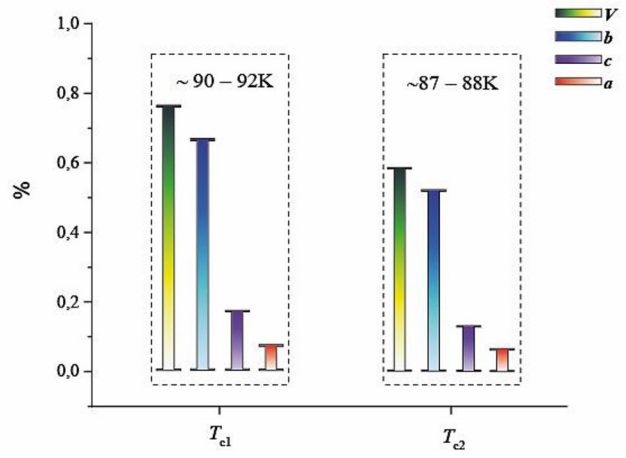

Fig. 9 Change in lattice parameters in the interval of transition to the superconducting state for two dominant superconducting phases

3.3 Unusual lattice dynamics

Unlike classical superconductors and normal metals, HTSC materials have a crystalline structure with lattice sizes of up to several tens of angstroms. They are characterized by a layered structure exhibiting significant anisotropy of properties [32, 33, 34, 36], anomalies of the phonon spectrum [9, 17, 42, 44], singularities of elastic and acoustic properties [10, 12, 13, 19, 49, 50, 51, 52], especially near Tc [12, 13, 43, 53, 54, 55]. Figure 9 shows the results of changes (in %) in the lattice parameters and volume from temperature in the region of the transition to the superconducting state. The values ($\Delta \boldsymbol{a}_s$, $\Delta \boldsymbol{b}_s$, $\Delta \boldsymbol{c}_s$ and ΔV_s) during the transition to the superconducting state were estimated using the expression $((x_{max}\text{-}x_{min})/x_0)$ 100%, where x_{max} and x_{min} are the maximum and minimum values for the transition regions T_{c1} and T_{c2} (for two dominant superconducting phases, see Fig. 8). The change in volume $\Delta \boldsymbol{V}$s in the temperature range from ~92 to ~90.5 K (T_{c1}) is approximately 1.2 times higher than for the interval from ~88 to ~87 K (T_{c2}) and is 0.73% and 0.58%, respectively. In this case, the change in parameter $\Delta \boldsymbol{b}_s$ (0.67% at T_{c1} and 0.5% at T_{c2}) exceeds the change in parameter $\Delta \boldsymbol{c}_s$ (~0.13% for both phases) by almost 4–5 times. As can be seen, the expansion of the lattice along the ***a*** direction, in contrast to the ***b*** and ***c*** directions, is insignificant, i.e. the value of $\Delta \boldsymbol{a}_s$ is only ~ 0.05% for T_{c1} and 0.06% for T_{c2}, respectively.

The negative thermal expansion (NTE) characteristic of HTSC materials is a result of the unusual dynamics of their lattice. The interaction between individual atoms or groups of atoms in such structures is highly anisotropic. The amplitude of atomic oscillations is significantly higher along the direction of the weak bond normal to the planes (chains) than along the direction of the planes where the bond is strong enough. This local anisotropy leads to a noticeable mean-square displacement of atoms from individual layers along different directions of the crystals. As a result of such displacement of atoms in the direction of the weak bond, the distance between atoms within the layer increases. Ultimately, an intralayer compressive force proportional to the displacement arises, leading to anisotropic negative expansion, similar to the "membrane effect" [56]. The authors in [57] theoretically showed that this effect is due only to the presence of high anisotropy of interatomic interaction. Since complexes of ions (for example, Cu and O) with different electron states differ in the rigidity of the bonds, the oscillations of the ion that unites them are anharmonic. In this case, the oscillation potential of such an ion is asymmetric, i.e. the equilibrium position is shifted toward a more rigid bond. When modeling the anharmonic behavior of oscillations in HTSC materials at low temperatures, the best fit is obtained by using a double-well potential as the oscillation potential of atoms. Tunneling of an ion between the wells leads to a dynamic charge exchange between these complexes (CuO_6). The frequency of charge exchange affects the frequency of interwell tunneling of the potential. Near T_c, at the onset of structural anomalies, the frequency of ion tunneling between the wells increases sharply [58, 59]. This fact suggests a connection between fluctuations in the superconductivity state and nonlinear phonons. In [60], the coordinates of atoms and the degree of splitting of double cation-anionic layers of CuO_2 were determined as a function of temperature and oxygen content. It was shown that with decreasing temperature, the dispersion of splitting of such layers decreases sharply, which ensures the fixation of a certain equilibrium structural state in the material, leading to a negative thermal expansion.

The authors in [61] note that the lattice anomalies are caused by the dynamic, rather than static, nature of the splitting of the Cu-O bond in the CuO_2 plane. In this case, oscillations of oxygen ions in a double-well potential are a common property for all superconductors with a perovskite lattice.

In [62], the electron configurations of atoms of distorted lattices corresponding to different temperatures were calculated for the compounds $YBa_2Cu_3O_7$, $HgBa_2CuO_4$ and $Bi_2Sr_2CaCu_2O_8$. It was found that such distortions are responsible for the expansion of the band and modification of the Fermi surface. The observed thermal expansion anomalies at low temperatures are a fundamental property for many superconductors with a perovskite structure (Figs. 5 and 9). Since they are accompanied by large changes in volume [63], it can be assumed that superstructural charge ordering occurs in the oxygen sublattice (charge density waves), which makes it possible to stabilize the lattice instability [64]. In [65], the compression of the lattice in HTSCs is explained by the energy gain during the transition to the superconducting

state [66]. Near T_c, an interesting effect is observed, caused by a type of electron instability (electron effect), associated with the volume dependence of the energy of superconducting condensation [67]. Therefore, the sensitivity of the electron band structure to minor changes in the structure is the reason for the observed high sensitivity of T_c to such structural changes [67]. Indeed, E.V. Antipov and co-authors in [68] showed that the elongation of the apical Cu-O bond correlates with T_c - the greater the length of the apical bond, the higher T_c.

The authors of this paper consider the $YBa_2Cu_3O_y$ lattice as a system of interacting polarized atoms, for which [57] along with the ionic type of bonding, a dispersion bond is characteristic, caused by London forces at small interatomic distances. A decrease in interatomic distances suggests a high degree of splitting of the allowed energy levels for charge excitations. According to the ideas of J. Slater [69], the self-organization of polarized interacting atoms with the corresponding charge excitations in them provides dielectric screening and chemical stability. The low inertia of these charge excitations increases the probability of their socialization and acquisition of their own energy spectrum, obeying the Pauli principle. Obviously, these considerations are confirmed by the results of the analysis of the correlation of the temperature dependences of the electrical resistance and thermal expansion coefficient of YBCO, presented in this work, especially in the interval of the transition to the superconducting state (Fig. 7). To establish the nature of superconductivity, it is necessary to carry out precision studies in the superconducting state using diffraction and dilatometry methods on the same YBCO samples.This includes setting the oxygen stoichiometry and determining the number of phases by using oxygen, including the underdoped state.

4 Conclusion

The results are presented demonstrating a close correlation between the electrical resistance and lattice distortions of YBCO, depending on temperature. The maximum value of YBCO samples obtained in three stages and showing signs of preferential crystallite orientation, the value of j_c at 82 K is ~421 A/cm^2. The onset of the transition to the superconducting state in the dependence of $d\rho/dT$ on T coincides with the onset on the $\alpha_V(T)$ curve and, thus, confirms the interpretation of negative thermal expansion as a consequence of electron condensation. It is shown that the changes in the value of Δa, in contrast to the parameters Δb and Δc, are almost two times smaller and amount to ~0.12%, which is characterized as anisotropic expansion. The dependences of $\alpha_\rho(T)$ on $\alpha_V(T)$ for two intervals are close to linear with correlation coefficients r to the pseudogap state of ~0.992 and in the pseudogap state of ~0.977. Irregularities in the form of maxima and minima of the functions are observed on the curves, the number of which is consistent with the changes (with extremum points) in the dependence of $d\rho/dT$ on T. It is found that for samples containing several superconducting phases of different stoichiometry, during the transition to the superconducting state up to Tc, compression is observed, followed by a positive volume jump for each phase. The observed anomalies of thermal expansion at low temperatures are a fundamental property for superconductors with perovskite structure.

Acknowledgements The authors thank the laboratory of the Institute of Solid State Physics of the Russian Academy of Sciences for carrying out X-ray structural measurements. During the work, the equipment of the Nanotechnology Research Center was used.

Author contributions A.E. Rabadanova: conceptualization, writing - original draft, methodology. S.Kh. Gadzhimagomedov: investigation, conceptualization, formal analysis. D.K. Palchaev: methodology, supervision. M.Kh. Rabadanov: formal analysis, validation. R.M. Emirov: investigation, validation. V.S. Efimchenko: investigation. Zh.Kh. Murlieva: formal analysis, validation; Sh.P. Faradzhev: investigation, validation. N.M.-R. Alikhanov: translation, validation.

Funding The work was carried out with the financial support of the Russian Foundation for Basic Research No. 20-32-90170 and State assignment FZNZ-2020-0002.

Data availability All the data generated or analysed during this study are included in this published article.

Declarations

Conflict of interest The authors disclose no competing interests.

References

1. H. Thomas, A. Marian, A. Chervyakov, S. Stückrad, C. Rubbia, Efficiency of superconducting transmission lines: an analysis with respect to the load factor and capacity rating. Electr. Power Syst. Res. **141**, 381–391 (2016)
2. S.K. Shrivastava, G. Kumar, Application of high-Tc superconducting Josephson junction devices. Int. J. Emerg. Technol. Innovative Res. (JETIR), **6**(1) (2019)
3. P. Giraldo-Gallo, J.A. Galvis, Z. Stegen, K.A. Modic, F.F. Balakirev, J.B. Betts, X. Lian, C. Moir, S.C. Riggs, J. Wu, A.T. Bollinger, X. He, I. Bozovic, B.J. Ramshaw, R.D. McDonald, G.S. Boebinger, A. Shekhter, Scale-invariant magnetoresistance in a cuprate superconductor. Science. **361**(6401), 479–481 (2018)
4. B. Keimer, S.A. Kivelson, M.R. Norman, S. Uchida, J. Zaanen, From quantum matter to high-temperature superconductivity in copper oxides. Nature. **518**(7538), 179 (2015)
5. F.S. Wells, A.V. Pan, X.R. Wang, S.A. Fedoseev, H. Hilgenkamp, Analysis of low-field isotropic vortex glass containing vortex groups in $YBa_2Cu_3O_{7-x}$ thin films visualized by scanning SQUID microscopy. Sci. Rep. **5**(1), 8677 (2015)
6. R.J. Cava, A.W. Hewat, E.A. Hewat, B. Batlogg, M. Marezio, K.M. Rabe, J.J. Krajewski, W.F. Jr Peck, L.W. Jr Rupp, Structural

anomalies, oxygen ordering and superconductivity in oxygen deficient $Ba_2YCu_3O_x$. Phys. C: Superconductivity. **165**(5–6), 419–433 (1990)
7. C. Krüger, K. Conder, H. Schwer, E. Kaldis, The dependence of the lattice parameters on oxygen content in orthorhombic $YBa_2Cu_3O_{6+x}$: a high precision reinvestigation of near equilibrium samples. J. Solid State Chem. **134**(2), 356–361 (1997)
8. J.L. Tallon, C. Bernhard, H. Shaked, R.L. Hitterman, J.D. Jorgensen, Generic superconducting phase behavior in high-T c cuprates: T c variation with hole concentration in $YBa_2Cu_3O_{7-\delta}$. Phys. Rev. B **51**(18), 12911 (1995)
9. R. Srinivasan, K.S. Girirajan, V. Ganesan, V. Radhakrishnan, G.S. Rao, Anomalous variation of the c lattice parameter of a sample of $YBa_2Cu_3O_{7-\delta}$ through the superconducting transition. Phys. Rev. B **38**(1), 889 (1988)
10. C. Meingast, V. Pasler, P. Nagel, A. Rykov, S. Tajima, P. Olsson, Phase fluctuations and the pseudogap in $YBa_2Cu_3O_x$. Phys. Rev. Lett. **86**(8), 1606 (2001)
11. Z.J. Yang, M. Yewondwossen, D.W. Lawther, S.P. Ritcey, D.J.W. Geldart, R.A. Dunlap, Thermal expansion of $Bi_{2.2}Sr_{1.8}CaCu_2O_x$ superconductor single crystals. J. Supercond. **8**(2), 233–239 (1995)
12. V. Pasler, P. Schweiss, C. Meingast, B. Obst, H. Wühl, A.I. Rykov, S. Tajima, 3D–XY critical fluctuations of the Thermal Expansivity in Detwinned $YBa_2Cu_3O_{7-\delta}$ single crystals near optimal doping. Phys. Rev. Lett. **81**(5), 1094–1097 (1998)
13. O. Kraut, C. Meingast, G. Bräuchle, H. Claus, A. Erb, G. Müller-Vogt, H. Wühl, Uniaxial pressure dependence of tc of untwinned $YBa_2Cu_3O_x$ single crystals for x = 6.5–7. Phys. C: Superconductivity. **205**(1–2), 139–146 (1993)
14. Y. Fujii, Y. Soejima, A. Okazaki, I.K. Bdikin, G.A. Emel'Chenko, A.A. Zhokhov, The characteristics of orthorhombicity of $YBa_2Cu_3O_{7-\delta}$ in superconducting state. Phys. C: Superconductivity. **377**(1–2), 49–55 (2002)
15. C. Uher, Thermal conductivity of high-T c superconductors. J. Supercond. **3**, 337–389 (1990)
16. V. Palmisano, S. Agrestini, G. Campi, M. Filippi, L. Simonelli, M. Fratini, Margiolaki I. Anomalous Thermal Expansion in Superconducting $Mg_{1-x}Al_xB_2$ system. J. Supercond. **18**(5), 737–741 (2005)
17. S.V. Pryanichnikov, S.G. Titova, L.A. Cherepanova, G.A. Dorogina, Anomalies of the crystal structure $Y_{1-x}Ca_xBa_2Cu_3O_y$ in the temperature region 80–300 K. Solid State Phys. **53**(10), 1889–1894 (2011)
18. S.G. Titova, V.A. Fotiev, A.V. Pashchenko, A.M. Burkhanov, V.V. Gudkov, I.V. Zhevstovskikh, A.V. Tkach, V.V. Ustinov SFHT. **4**, 1010 (1991)
19. S.G. Titova, T.I. Arbuzova, V.F. Balakirev, O.M. Fiodorova, P.P. Pal-Val, L.N. Pal-Val, Anomalies of magnetic and acoustic properties and structure parameters of ceramic HTS materials in the temperature range 100–300 K. Fiz. Niz Temp. **22**(10), 1231–1232 (1996)
20. C. Meingast, O. Kraut, T. Wolf, H. Wühl, A. Erb, G. Müller-Vogt, Large a-b anisotropy of the expansivity anomaly at T_c in untwinned $YBa_2Cu_3O_{7-\delta}$. Phys. Rev. Lett. **67**(12), 1634 (1991)
21. M. Francois, A. Junod, K. Yvon, A.W. Hewat, J.J. Capponi, P. Strobel et al., A study of the Cu-O chains in the high T_c superconductor $YBa_2Cu_3O_7$ by high resolution neutron powder diffraction. Solid State Commun. **66**(10), 1117–1125 (1988)
22. X.S. Wu, S. Nie, F.Z. Wang, Y. Ding, S.S. Jiang, J. Gao, Structural changes of $Y_{0.8}Ca_{0.2}Ba_{1.8}La_{0.2}Cu_3O_y$ at low temperature. Phys. C: Superconductivity. **340**(2–3), 185–192 (2000)
23. G. Deutscher, The role of Cu-O bond length fluctuations in the high temperature superconductivity mechanism. J. Appl. Phys., **111**(11) (2012)
24. C.H. Booth, F. Bridges, J.B. Boyce, T. Claeson, B.M. Lairson, R. Liang, D.A. Bonn, Comparison of local structure measurements from *c*-axis polarized XAFS between a film and a single crystal of $YBa_2Cu_3O_{7-\delta}$ as a function of temperature. Phys. Rev. B **54**(13), 9542 (1996)
25. H. Maruyama, T. Ishii, N. Bamba, H. Maeda, A. Koizumi, Y. Yoshikawa, H. Yamazaki, Temperature dependence of the EXAFS spectrum in $YBa_2Cu_3O_{7-\delta}$ compounds. Phys. C: Superconductivity. **160**(5–6), 524–532 (1989)
26. S. Gupta, G. Bera, M. Dhanetwal, D. Prajapat, R. Mirshahi, A. Upadhyay et al., Study of spin-phonon coupling and site-disorder in polycrystalline $YBaCuFeO_5$. Phys. Rev. Mater. **8**(11), 114414 (2024)
27. S.K. Gadzhimagomedov, D.K. Palchaev, Z.K. Murlieva, M.K. Rabadanov, M.Y. Presnyakov, E.V. Yastremsky, N.S. Shabanov, R.M. Emirov, A.E. Rabadanova, YBCO nanostructured ceramics: relationship between doping level and temperature coefficient of electrical resistance. J. Phys. Chem. Solids. **168**, 110811 (2022)
28. Y. Zhang, X. Xu, Yttrium barium copper oxide superconducting transition temperature modeling through gaussian process regression. Comput. Mater. Sci. **179**, 109583 (2020)
29. Y. Zhang, X. Xu, Predicting doped MgB_2 superconductor critical temperature from lattice parameters using gaussian process regression. Physica C (Amsterdam, Neth.). **573**, 1353633 (2020)
30. W. Matz, L. Weiss, G. Schuster, E.S. Kuklina, Nozik Yu Z. Soviet Phys. Crystallogr. **36**, 125–126 (1991)
31. P. Benzi, E. Bottizzo, N. Rizzi, Oxygen determination from cell dimensions in YBCO superconductors. J. Cryst. Growth. **269**(2–4), 625–629 (2004)
32. S.L. Bud'ko, M.F. Davis, J.C. Wolfe, C.W. Chu, P.H. Hor, Pressure and temperature dependence of the critical current density in $YBa_2Cu_3O_{7-\delta}$ thin films. Phys. Rev. B **47**(5), 2835 (1993)
33. E.D. Specht, A. Goyal, J. Li, P.M. Martin, X. Li, M.W. Rupich, Stacking faults in $YBa_2Cu_3O_{7-x}$: measurement using x-ray diffraction and effects on critical current. Appl. Phys. Lett., **89**(16) (2006)
34. S.P.K. Naik, P.M.S. Raju, T. Rajasekharan, V. Seshubai, Relevance of nanosized defects to hardness and current density of YBCO superconducting composites. IEEE Trans. Appl. Supercond. **26**(8), 1–6 (2016)
35. A.E. Rabadanova, D.K. Palchaev, M.K. Rabadanov, S.K. Gadzhimagomedov, M.Z.K. Emirov, R.M. Alikhanov, Effect of Heat Treatment on changes in the structure of YBCO superconducting powders. HERALD Dagestan State Univ. **36**(3), 37–50 (2021)
36. E.F. Talantsev, N.M. Strickland, S.C. Wimbush, J.G. Storey, J.L. Tallon, Long N.J. Hole doping dependence of critical current density in $YBa_2Cu_3O_{7-\delta}$ conductors. Appl. Phys. Lett., **104**(24) (2014)
37. K.S. Pigalskiy, L.G. Mamsurova, A.A. Vishnev, S.Kh. Gadzhimagomedov, Zh.Kh. Murlieva, DK. Palchaev, A. S. Bugaev. Magnetodynamic studies of fine-crystalline samples of high-temperature superconductors $YBa_2Cu_3O_y$ synthesized by the sol–gel method. Russian Journal of Physical Chemistry B. **12**(6), 1024–1030 (2018)
38. A. Harabor, P. Rotaru, N.A. Harabor, P. Nozar, A. Rotaru, Orthorhombic YBCO-123 ceramic oxide superconductor: Structural, resistive and thermal properties. Ceram. Int. **45**(2), 2899–2907 (2019)
39. V.D. Mote, Y. Purushotham, B.N. Dole, Williamson-Hall analysis in estimation of lattice strain in nanometer-sized ZnO particles. J. Theoretical Appl. Phys. **6**, 1–8 (2012)
40. E.A. Belenkov, D.V. Iakovlev, Peculiarities of the analysis of the form of profiles x–ray diffraction lines for carbon materials. Part ii. Relation of the form of profiles and distribution of crystals on the sizes. News Chelyabinsk Sci. Cent. **2**(11), 38–45 (2001)

41. Y. Xue, H. Kaneko, Q. Tao, Z. Xu, N. Takeda, Y. Nemoto, T. Goto, H. Suzuki, Low temperature x-ray diffraction study on superconductivity. *Journal of Physics: Conference Series* 150(5), 052284 (2009)
42. L. Sun, Y. Wang, H. Shen, X. Cheng, Effect of structural instability between 80 and 300 K on superconductivity of $YBa_2Cu_3O_x$. Phys. Rev. B **38**(7), 5114 (1988)
43. H. Zhang, Y. Zhao, Q.R. Feng, S.G. Wang, F. Ritter, W. Assmus, A structure anomaly in $YBa_2Cu_3O_{7-x}$ and $PrBa_2Cu_3O_{7-x}$ polycrystals. Solid State Commun. **97**(2), 149–152 (1996)
44. S.G. Titova, A.V. Lukoyanov, S.V. Pryanichnikov, L.A. Cherepanova, A.N. Titov, Crystal and electronic structure of high temperature superconducting compound $Y_{1-x}Ca_xBa_2Cu_3O_y$ in the temperature interval 80–300 K. J. Alloys Compd. **658**, 891–897 (2016)
45. S.G. Titova, A.S. Shkvarin, A.V. Lukoyanov, S.V. Pryanichnikov, R.G. Chumakov, A.M. Lebedev, L.P. Kozeeva, M.Y. Kameneva, Fedorov V.E. ARPES Study of Localized Charge Carriers in $Y_{0.9}Ca0._1Ba_2Cu_3O_{6.8}$ high-temperature superconductor. J. Supercond. Novel Magn. **36**(4), 1093–1096 (2023)
46. A.Y. Gufan, Y.V. Prus, On the origin of orthorhombic deformations in $YBa_2Cu_3O_{7-y}$. Phys. Solid State. **42**, 1211–1214 (2000)
47. G.G. Gridneva, O.A. Bunina, O.F. Bazaev, V.S. Filipev, Superconductivity: physics, chemistry, technology 4(9) 1734 (1991)
48. Y. Sun, G. Strasser, E. Gornik, W. Seidenbusch, W. Rauch, Critical temperature dependence of $YBa_2Cu_3O_y$ and $Y_{1-x}Ca_xBa_2Cu_3O_y$ on carrier concentration. Phys. C: Superconductivity. **206**(3–4), 291–296 (1993)
49. C. Stari, A. Moreno-Gobbi, A.W. Mombru, S. Sergeenkov, A.J.C. Lanfredi, C.A. Cardoso, F.M. Araujo-Moreira, Elastic properties of polycrystalline $YBa_2Cu_3O_{7-\delta}$: evidence for granularity induced martensitic behavior. Phys. C: Superconductivity. **433**(1–2), 50–58 (2005)
50. V.N. Nikiforov, N.A. Bulychev, V.V. Rzhevsky, Elastic properties of HTSP ceramics. Brief. Commun. Phys. FIAN. **43**(2), 39–47 (2016)
51. P.P. Pal-Val, L.N. Pal-Val, V.V. Demirsky, V.D. Natsik, M.N. Sorin, Anisotropy of elastic and relaxation properties of the superconducting 123-YBCO single crystal. Le J. De Phys. IV. **6**(C8), C8–489 (1996)
52. H. Kamioka, N.O.N. Okuda, S.N.S. Nitta, Elastic anomalies of High-T_c Superconductor $YBa_2Cu_3O_{7-x}$ between 77 K and 300 K. Jpn. J. Appl. Phys. **30**(6R), 1204 (1991)
53. A.I. Korobov, A.I. Kokshaiskii, N.V. Shirgina, N.I. Odina, A.A. Agafonov, Rzhevskii V.V. Shear elastic properties of HTSC ceramics in the region of superconducting transition. Tech. Phys. **65**, 914–920 (2020)
54. H. You, U. Welp, Y. Fang, Slope discontinuity and fluctuation of lattice expansion near T_c in untwinned $YBa_2Cu_3O_{7-\delta}$ single crystals. Phys. Rev. B **43**(4), 3660 (1991)
55. W. Schnelle, E. Braun, H. Broicher, R. Dömel, S. Ruppel, W. Braunisch, J. Harnischmacher, D. Wohlleben, Fluctuation specific heat and thermal expansion of YBaCuO and DyBaCuO. Phys. C: Superconductivity. **168**(5–6), 465–474 (1990)
56. V. Eremenko, S. Feodosyev, I. Gospodarev, V. Ibulaev, R.W. McCallum, M. Shvedun, V. Sirenko, Negative expansion of $Eu(Ba_{1-x}La_x)_2Cu_3O_{7-d}$ compounds. In *AIP Conference Proceedings*, 850(1), 489–490 (2006)
57. S.B. Fedos' ev, E.S. Syrkin, I.A. Gospodarev, Low temperature peculiarities of thermal expansion of laminated crystals. Fiz. Tverd. Tela. **31**(1), 186–194 (1989)
58. De J.M. Leon, S.D. Conradson, I. Batistić, A.R. Bishop, Evidence for an axial oxygen-centered lattice fluctuation associated with the superconducting transition in $YBa_2Cu_3O_7$. Phys. Rev. Lett. **65**(13), 1675 (1990)
59. J.M. De León, I. Batistić, A.R. Bishop, S.D. Conradson, S.A. Trugman, Polaron origin for anharmonicity of the axial oxygen in $YBa_2Cu_3O_7$. Phys. Rev. Lett. **68**(21), 3236 (1992)
60. O.M. Fedorova, S.G. Titova, A.M. Yankin, V.F. Balakirev, Negative thermal expansion coefficient in HTSC material $Bi_2Sr_2CaCu_2O_\gamma$. *News of the russian academy of sciences. Physics series*, 2005, 69(7), 1049–1051, (2005)
61. A. Menushenkov, Correlation of the local and the macroscopic properties of high-temperature superconductors: EXAFS data analysis. J. Synchrotron Radiat. **10**(5), 369–370 (2003)
62. T. Jarlborg, G. Santi, The role of thermal disorder on the electronic structure in high-T_c compounds. Phys. C: Superconductivity. **329**(4), 243–257 (2000)
63. da M.S. Luz, J.J. Neumeier, R.K. Bollinger, A.S. Sefat, M.A. McGuire, R. Jin, B.C. Sales, D. Mandrus, High-resolution measurements of the thermal expansion of superconducting co-doped $BaFe_2As_2$. Phys. Rev. B **79**(21), 214505 (2009)
64. N.V. Anshukova, A.I. Golovashkin, L.I. Ivanova, I.B. Krynetsky, A.P. Rusakov, Anomalous thermal expansion of the $Bi_2Sr_{2-x}La_xCuO_6$ HTSC system at low temperatures. Solid State Phys. **48**(8), 1358–1365 (2006)
65. K.Y.V. Golovashkin, A.I. Anshukova et al., N.V. // Fifth Int. conf. new theories, discoveries and applications of superconductors and related materials (New3SC(5). Peking, China. 2004. P. 56
66. I.B. Krynetsky, A.I. Golovashkin, A.P. Rusakov, V.P. Martovitsky, S.Y. Gavrilkin, V.I. Kovalenko, N.P. Shabanova, Anomalies of thermal expansion of high temperature superconductor $Bi_2Sr_{2-x}La_xCuO_{6+\delta}$ in the dielectric phase ($x \geq 0.8$) and charge ordering in the oxygen sublattice. Bull. Russian Acad. Sciences: Phys. **75**(8), 1077–1079 (2011)
67. F. Hardy, P. Adelmann, H.V. Löhneysen, T. Wolf, C. Meingast, Large anisotropic uniaxial pressure dependencies of tc in single crystalline $ba(Fe_{0.92}Co_{0.08})_2As_2$. Phys. Rev. Lett. **102**, 187004 (2009)
68. E.V. Antipov, A.M. Abakumov, S.N. Putilin, Synthesis and structure of Hg-based superconducting cu mixed oxides. Supercond. Sci. Technol. **15**, R1–R19 (2002)
69. J.C. Slater, Insulators, *Semiconductors and Metals* (McGraw-Hill, New York, 1967), p. 647